THEORY OF A MAGNETIC LENS TYPE BETA RAY SPECTROMETER

by N. F. VERSTER

Institute for Nuclear Research, Zeeman Laboratory, Amsterdam

Summary

The behaviour of the electrons near the focal plane is investigated in the case of a lens type beta ray spectrometer with arbitrary field shape. Spherical and chromatic aberration constants are introduced. After some approximations a simple formula results, showing the existence of a well defined ring shaped focus. A formula for the influence of the earth's magnetic field on the lens strength is given. The theoretical results are compared with measurements, carried out with a short lens spectrometer. A procedure for the alignment of the magnetic lens is described.

§ 1. *Introduction.* Several aspects of the theory of lens type beta ray spectrometers have been dealt with by various authors. A short lens spectrometer is described by Deutsch, Elliot and Evans[1]). The transmission and the resolving power are calculated from the measured or calculated value of the spherical aberration. The chromatic aberration is deduced from the properties of a thin optical lens. The influence of the field shape on the spherical aberration is dealt with by K. Siegbahn[2]). A lens spectrometer with a special field shape and very low spherical aberration is described by the same author[3]). A solenoid type spectrometer is described by Witcher[4]). This spectrometer uses a ring shaped focusing slit. A theory of the transmission and resolution is given. This type of spectrometer has been treated recently by Dumond[5]) and by Persico[6]). Both authors have dealt with the problem of the optimum design of such a spectrometer using a ring shaped focusing slit. Recently a lens type spectrometer, also using this kind of focusing, has been announced by Zünti[7]).

In this paper we discuss the spherical and chromatic aberration of a magnetic lens with arbitrary field shape, covering also the solenoid type as a special case. In part I our calculation of the third order spherical and chromatic aberration of a magnetic lens with axial symmetry is shown to lead to convenient formulae describing the behaviour of the electrons in the vicinity of the focal plane. The formulae derived show clearly the existence of a well defined ring shaped focus near the focal plane. In the course of the calculations suitable approximations are introduced; the influence of these approximations on the resulting formulae can be easily estimated in any special case. Our formulae allow the calculation of the transmission and resolution and can be used as a starting-point for further investigations of lens type spectrometers using a ring focus. By treating the axial component of the earth's magnetic field (or any other weak stray field) as a perturbation, a formula giving the influence of such a, not necessarily homogeneous, field is derived along the same lines. In part II we compare some of our theoretical results with measurements carried out with a short magnetic lens spectrometer, recently built by us.

PART I

§ 2. *The ray equation.* We use cylindrical coordinates r, φ, z; z being the symmetry axis of the magnetic field.

The ray equation can be derived from the Langrangian equation

$$\frac{d}{dt}\frac{\partial L}{\partial \dot{\varphi}} - \frac{\partial L}{\partial \varphi} = 0, \quad L = \tfrac{1}{2}\, mv^2 + (\mathbf{vA}) \tag{1}$$

and the principle of Maupertuis

$$\delta \int_a^b [mv + e\,(\mathbf{sA})]\, ds = 0, \tag{2}$$

where e is the charge of the particle in e.m.u., $\mathbf{A}$ the vector potential in Gcm and $\mathbf{s} = \mathbf{v}/v$. A_r and A_z both vanish in the case of normal lens construction with axial symmetry. A_φ will be denoted by A.

From (1) we find, due to the axial symmetry,

$$P_\varphi = mr^2\dot{\varphi} + erA = C. \tag{3}$$

We will confine ourselves to particles starting from a point on the axis; then (3) reduces to

$$P_\varphi = mr^2\dot{\varphi} + erA = 0 \quad \text{or} \quad r\dot{\varphi} = -\, vA/H\varrho. \tag{4}$$

The symbol $H\varrho$ is used to describe the momentum of the particles and is given by

$$H\varrho = mv/e.$$

By using (4), equation (2) can be transformed into

$$\delta \int_a^b [1 - (A/H\varrho)^2]^{\frac{1}{2}} \, ds = 0 \tag{5}$$

or

$$\delta \int_a^b [1 - (A/H\varrho)^2]^{\frac{1}{2}} \, (1 + r'^2)^{\frac{1}{2}} \, dz = 0, \tag{6}$$

where r' stands for dr/dz.

Equation (5) shows that our problem is identical with a two-dimensional optical problem, with a refractive index proportional to $[1 - (A/H\varrho)^2]^{\frac{1}{2}}$. Equation (6) is identical with the differential equation [8]).

$$r'' = -\frac{(1 + r'^2)(\partial A^2/\partial r - r'\partial A^2/\partial z)}{2H\varrho^2[1 - (A/H\varrho)^2]} \,. \tag{7}$$

As a result of the field equation curl curl $\mathbf{A} = 0$ and the assumed axial symmetry, $A (= A_\varphi)$ can be expanded in a power series [9])

$$A = \sum_0^\infty (-1)^n \frac{H(z)^{(2n)}}{n!(n+1)!} \frac{r^{2n+1}}{2^{2n+1}} = \frac{H(z)}{2} r - \frac{H''(z)}{16} r^3 + \ldots \tag{8}$$

$H(z)$ is the magnetic field strength along the axis, $H^{(2n)}$ denotes $d^{2n}H(z)/dz^{2n}$.

Substituting (8) in (7), the right hand side of equation (7) can be expanded in a power series

$$-r'' = \frac{1}{4\,H\varrho^2} [rH^2 + r^3(H^2r'^2/r^2 - HH'r'/r - HH''/2 + \\ + H^4/4H\varrho^2) + r^5 \ldots]. \tag{9}$$

We now introduce k by

$$k = i/2H\varrho \tag{10}$$

and $h(z)$, the magnetic field for unit current, by

$$h = H/i. \tag{11}$$

If we omit fifth and higher order terms, equation (9) becomes

$$r'' + k^2rh^2 + k^2r^3B = 0, \tag{12}$$

B being given by

$$B = k^2h^4 - hh''/2 - hh'r'/r + h^2(r'/r)^2. \tag{13}$$

The solution r_0 of the first order equation

$$r_0'' + k_0^2 r_0 h^2 = 0 \tag{14}$$

together with the boundary conditions

$$r_0(a) = r_0(b) = 0 \tag{15}$$

can be found quickly by stepwise numerical integration of (14) with successive approximations of k_0. As will be shown below (formula (23)) the influence of the value of k on $r(b)$ can be estimated.

Another method for solving (14, 15) is given by v. Ments and Le Poole[10]). Their method furnishes a series expansion of the solution of (14) in powers of k. This method might prove valuable for a short lens spectrometer using variable magnification. A method of solution for bell-shaped fields of the kind $h(z) = h_0\,(1 + (z/a)^2)^{-\mu}$ is described by Svartholm[11]).

§ 3. *Spherical and chromatic aberration* (fig. 1). To obtain a formula for the spherical and chromatic aberration we treat the third term in (12) as a perturbation and introduce a small variation in the parameter k. We compare the solution r_1 of

$$r_1'' + k_1^2\, rh^2 + k_1^2 r_1^3 B = 0, \tag{16}$$

restricted by $r_1(a) = 0$, $r_1'(a) = r_0'(a)$, with the solution r_0 of the first order equations (14, 15).

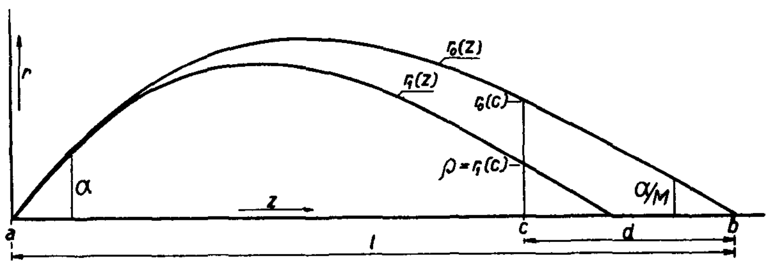

Fig. 1. A solution $r_0(z)$ of the first order equation and a corresponding solution $r_1(z)$ of the third order equation. By choosing an appropriate value of the parameter k_1, the condition $r_0 \approx r_1$ can be fulfilled.

Multiplication of (14) by r_1 and (16) by r_0, followed by substraction, yields

$$r_0 r_1'' - r_1 r_0'' + (k_1^2 - k_0^2) r_1 r_0 h^2 + k_1^2 r_1^3 r_0 B = 0.$$

Integration from the source position a to a point c in the neighbourhood of b gives

$$r_0'(c)r_1(c) = (k_1^2 - k_0^2)\int_a^c r_1 r_0 h^2\,dz + k_1^2\int_a^c r_0 r_1^3 B\,dz + r_1'(c)r_0(c). \quad (17)$$

This equation is an exact representation of the third order ray path. We now make some approximations to get (17) in a more convenient shape.

a) Let us suppose that the counter window is located at $z = b$. The difference between r_0 and r_1 can then be neglected in the integrals. (This would be immediately clear if the spherical aberration were deduced from (6)).

b) The second integral of (17) we change into

$$k_0^2\int_a^b r_0^4 B\,(r_0, k_0)\,dz.$$

This will greatly simplify the further treatment.

c) We put $r_0'(c) = r_1'(c) = r_0'(b)$ and $r_0(c) = -(b-c)r_0'(b) = -dr_0'(b)$.

As a special solution of (14, 15) we introduce $R(z)$ with $R'(a) = 1$; consequently

$$r_0(z) = \alpha R(z), \quad (18)$$

where α is the tangent of the exit angle ($\alpha = r_0'(a)$). Moreover we introduce the magnification M by means of

$$M = -r_0'(a)/r_0'(b) = -\alpha/r_0'(b), \quad (19)$$

the chromatic aberration constant C_1 by

$$C_1 = 2Mk_0^2\int_a^c R^2 h^2\,dz, \quad (20)$$

the spherical aberration constant C_2 by

$$C_2 = Mk_0^2\int_a^b R^4 B\,dz, \quad (21)$$

a quantity Δ, equal to the relative variation in momentum of the focused particles, by

$$\Delta = (k_0^2 - k_1^2)/2k_0^2 \quad (22)$$

and finally

$$\varrho = r_1(c).$$

We then obtain the formula

$$\varrho = \alpha d/M + \alpha\Delta C_1 - \alpha^3 C_2. \quad (23)$$

§ 4. *Discussion.* The influence of the source dimensions on the resolution is determined by C_1, the influence of the spherical aberration by C_2/C_1.

C_1 may be estimated with the aid of (14), which gives

$$Mk^2 \int_a^b Rh^2 \, dz = 1 + M.$$

In the case of a very short lens we get

$$2Mk^2 \int_a^b R^2h^2 \, dz = 2(b - a) = 2l, \tag{24}$$

in the case of a solenoid

$$2Mk^2 \int_a^b R^2h^2 \, dz = l. \tag{25}$$

The influence of the upper limit on C_1 can easily be estimated. Equation (23) with an estimated value of C_1 will be of use when solving the boundary problem (14, 15).

The value of C_2 greatly influences the performance of the instrument. Formula (22) can be transformed by partial integration [12]) to

$$C_2 = (Mk_0^2/12) \int_a^b R^4 \, [16k_0^2h^4 + 5h'^2 - hh''] \, dz. \tag{26}$$

In the case of a solenoid we find that $C_2 = l/2$. The value of C_2 for a short lens depends on the field shape, especially the half value width of $H(z)$. Values of C_2 of about $3l$ are normal. C_2 can be decreased below $l/2$ by using a field shape with a positive value of $H''(z)$ as done by Siegbahn [3]). A construction free of iron may be favourable for a precision instrument.

The fact that an important decrease of spherical aberration can be obtained by a moderate increase in copper $\times$ power is a strong argument in favour of this type of magnetic lens instead of the solenoid type.

It is to be noted that in the case of a solenoid spectrometer the values of C_1 and C_2 do not change if higher order focusing is used, i.e. if the electrons cross the axis one or more times before reaching the counter. The maximum value of R for a given exit angle and distance between source and counter is inversely proportional to the order of focusing, the required field strength is proportional to the order of focusing. The construction of a solenoid spectrometer using for high energy electrons the economic optimum exit angle of about 20° [6]), for medium and low energy electrons, however, an exit angle of about 45° [5]) [6]) and second order focusing seems advantageous. Higher order focusing moreover allows an important reduction of instrumental scattering by a suitable location of baffles, one being placed at the first nodal point.

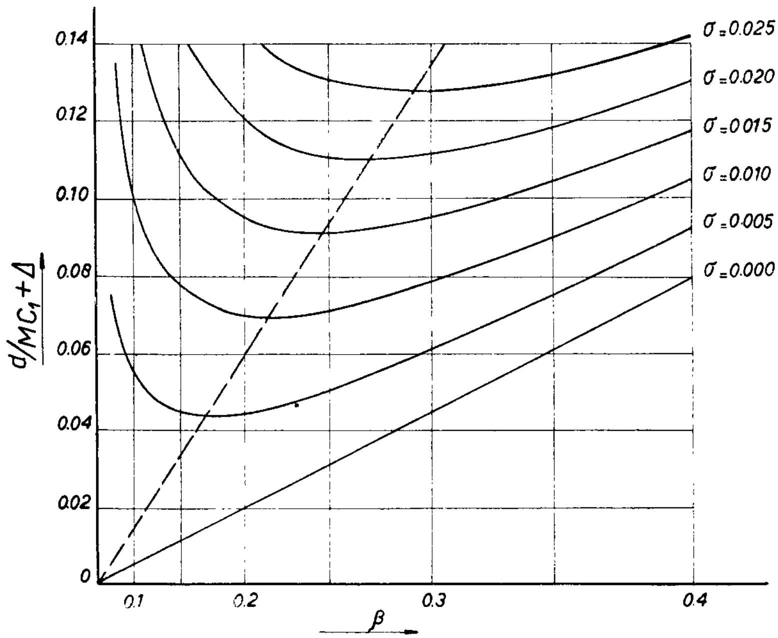

Fig. 2. A graphical representation of equation (23) with the substitutions $\sigma = \varrho(2C_2/C_1^3)^{\frac{1}{2}}$ and $\beta = \alpha(2C_2/C_1)^{\frac{1}{2}}$. This diagram clearly shows how the effect of the spherical aberration on the resolving power can be reduced by using a ring-shaped focusing slit ($\sigma > 0$).

§ 5. *The ringfocus.* Several authors have recently drawn attention to the existence of a ring-shaped focus of greater definition than the central focus in the image plane. This is particularly true for small solid angles. A theoretical treatment, however, has only been given for a solenoid spectrometer [4]) [5]) [6]). Practical applications are published by Witcher [4]) and by Zünti [7]). We make use of this ring focus in our spectrometer.

The properties of the ring focus can be derived from (23). The axial distance of the electrons in a plane $z = c$ must be independent of small variations in a:

$$\partial\varrho/\partial a = d/M + \Delta C_1 - 3a^2 C_2 = 0.$$

The coordinates of the ring focus will be indicated by an index f. We choose for d a value $d_f = M\varrho_f/a_f$ so that the electrons pass the axis near the counter window at $z = b$. The difference between $r_0(z)$ and $r_1(z)$ is then small. The position of the ring focus is now given by

$$\begin{aligned}\varrho_f &= a_f d_f M = 2a_f^3 C_2, \\ \Delta &= a_f^2 C_2/C_1.\end{aligned} \tag{27}$$

In the case of a solenoid spectrometer the coordinates of the ring focus can be calculated exactly. For an instrumental length of 100 cm and a homogeneous field our formula (27) reduces to $\varrho/a = d = 100\,a^2$, $2\Delta = 100\,a^2$ per cent.

A comparison is given in table I. The deviation of our approximate values from the exact values is given in per cent of the exact value. A deviation of the order of $100\,a^2$ per cent can be expected as our formula (27) only represents the first term of a series expansion in even powers of a. A calculation of the next term however requires a knowledge of $H^{IV}(z)$. As the value of this fourth derivative of the axial field strength $H(z)$ can generally not be obtained from a measurement of $H(z)$, a restriction to the simple formula (27) seems justified.

TABLE I

A comparison between (27) and the exact values in the special case of a solenoid spectrometer with an instrumental length of 100 cm. The deviation is in percent of the exact value.

a	d Exact values	d deviation	ϱ/a Exact values	ϱ/a deviation	2Δ Exact values	2Δ deviation	$100a^2$
0.1	0.99 cm	1 percent	0.99 cm	1 percent	0.99percent	1 percent	1
0.2	3.82 ,,	4.7 ,,	3.82 ,,	4.7 ,,	3.84 ,,	4 ,,	4
0.3	8.09 ,,	10 ,,	8.00 ,,	12.5 ,,	8.25 ,,	9 ,,	9
0.4	13.11 ,,	22 ,,	12.73 ,,	25.6 ,,	13.80 ,,	16 ,,	16
0.5	18.14 ,,	37 ,,	17.23 ,,	45 ,,	20.00 ,,	25 ,,	25
0.6	22.85 ,,	57 ,,	20.92 ,,	72 ,,	26.50 ,,	36 ,,	36

A series expansion of (23) in the region of the ring focus yields

$$\varrho - \varrho_f = (\Delta - \Delta_f)\, a_f C_1 + (d - d_f) a_f/M - (a - a_f)^2\, 3a_f C_2. \tag{28}$$

A graphical representation of (23) (fig. 2) may be useful to understand the behaviour of the rays near the focal plane. We have used the variables $\beta = \alpha(2C_2/C_1)^{\frac{1}{2}}$ and $\sigma = \varrho(2C_2/C_1^3)^{\frac{1}{2}}$. In the case of a solenoid one finds $\alpha = \beta$ and $\varrho = \sigma l$.

It is immediately clear from this figure that the variation in Δ for a given solid angle is less for a ring focus ($\sigma > 0$) than for a point focus ($\sigma = 0$). The transmission curve can be calculated from (28) in any specified case by the method described by D e u t s c h [1]).

§ 6. *Influence of the earth's magnetic field.* The influence of the axial component of the earth's magnetic field on the lens strength can be derived in the same way as the spherical and chromatic aberration. We assume a weak field H_e in the z direction, superposed on the field H produced by the lens coil.

Let R_0 and k_0 be the solution of the first order equation (14, 15) without earth field and R_1 and k_1 the solution with earth field. In first approximation we then have the equations

$$R_0'' + k_0^2 h^2 R_0 = 0,$$

$$R_1'' + k_1^2 h^2 R_1 + (2k_1^2/i_1)\, hH_e R = 0.$$

The method used to derive (17) now yields

$$(k_1^2 - k_0^2) \int_a^b R_0 R_1 h^2\, dz + (2k_1^2/i_1) \int_a^b R_0 R_1 h H_e\, dz = 0.$$

If we assume that $R_0 \approx R_1$ and $| k_1 - k_0 | \ll k_0$, we get for any value of $H\varrho$

$$i_1 - i_0 = -\frac{\int_a^b R_0^2 h H_e\, dz}{\int_a^b R_0^2 h^2\, dz}. \tag{29}$$

PART II

§ 7. *Description of the beta ray spectrometer.* A schematic cross-section of the spectrometer is shown in fig. 3. The vacuum chamber is 100 cm long and has a diameter of 30 cm. Counter and source can be separated from the vacuum by means of vacuum sluices. The instrumental axis is vertical. The source is placed at the bottom. The magnet consists of 5 flat double coils having each 2×50 turns of copper $6\frac{1}{4} \times 2\frac{1}{4}$ mm^2. The cooling is effected by flat watercooled copper tanks between the double coils. The dimensions of the magnet are: 17 cm i.d.; 34 cm o.d.; length 10 cm.

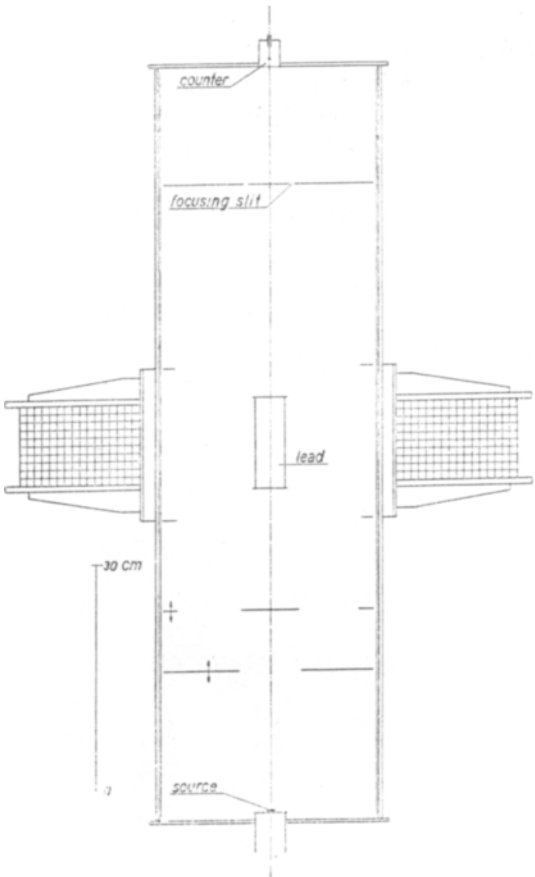

Fig. 3. A schematic cross-section of the spectrometer.

It is not unlikely that the spherical aberration of this lens can be reduced by dividing the magnet into two separate parts and placing these two parts at a certain distance from each other. Calculations are in progress to determine the effect of this change.

The maximum magnet current of 120 A makes it possible to focus 5 MeV electrons. The power dissipation at this current amounts to 15 kW. The electronic equipment used to stabilize the magnet current is discussed in a separate publication [13]).

§ 8. *Alignment of the lens.* The axis of symmetry of the magnetic field has to coincide exactly with the axis of the spectrometer. To obtain this alignment we made use of a rod, fixed accurately in the axis of the spectroscope and carrying a search coil (fig. 4). This

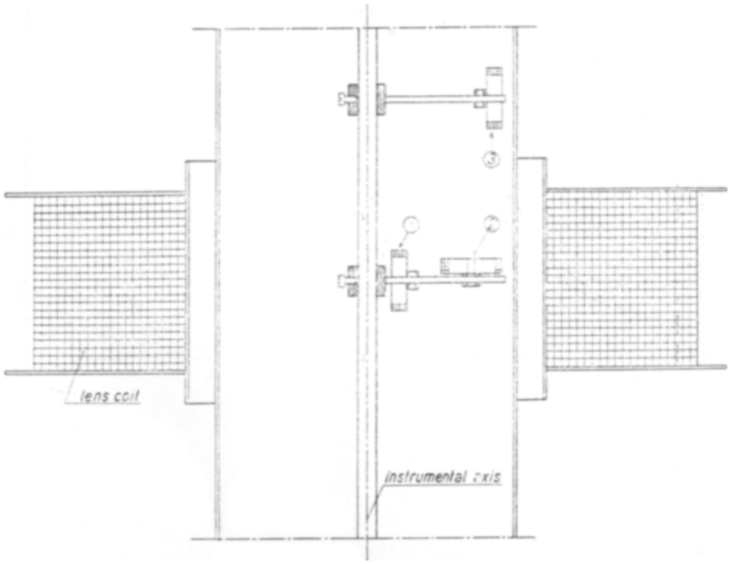

Fig. 4. The search coil used for the alignment of the magnet. Position (1) measures the tilt of the magnet. Position (2) measures the radial displacement. Position (3) has been used for control measurements.

search coil was connected to a creep galvanometer. If the alignment is perfect, no galvanometer deflection will result from a rotation of the rod. The following procedure has proved useful to obtain rapidly the required alignment.

1) Coil in position 1. The magnet is tilted until no galvanometer deflection results from a rotation of the rod.

2) Coil in position 2, measuring the field strength $H_z(r)$. Its value follows from (8):

$$H_z(r) = H_z(0) - \tfrac{1}{4}\, H_z''(0) \, . \, r^2.$$

The dependence on r makes it possible to determine the axis of symmetry of the magnetic field. The magnet is moved without changing the direction of its axis, until the galvanometer is again insensitive to a rotation of the rod. 1) and 2) are repeated until both conditions are fulfilled.

3) Coil in position 3, measuring $H_r(z)$. The value of the radial field strength as given by (8) is $H_r(r) = -H_z'(0)r/2$. The galvanometer has now also to be insensitive to a rotation of the rod. This can be used as a control measurement.

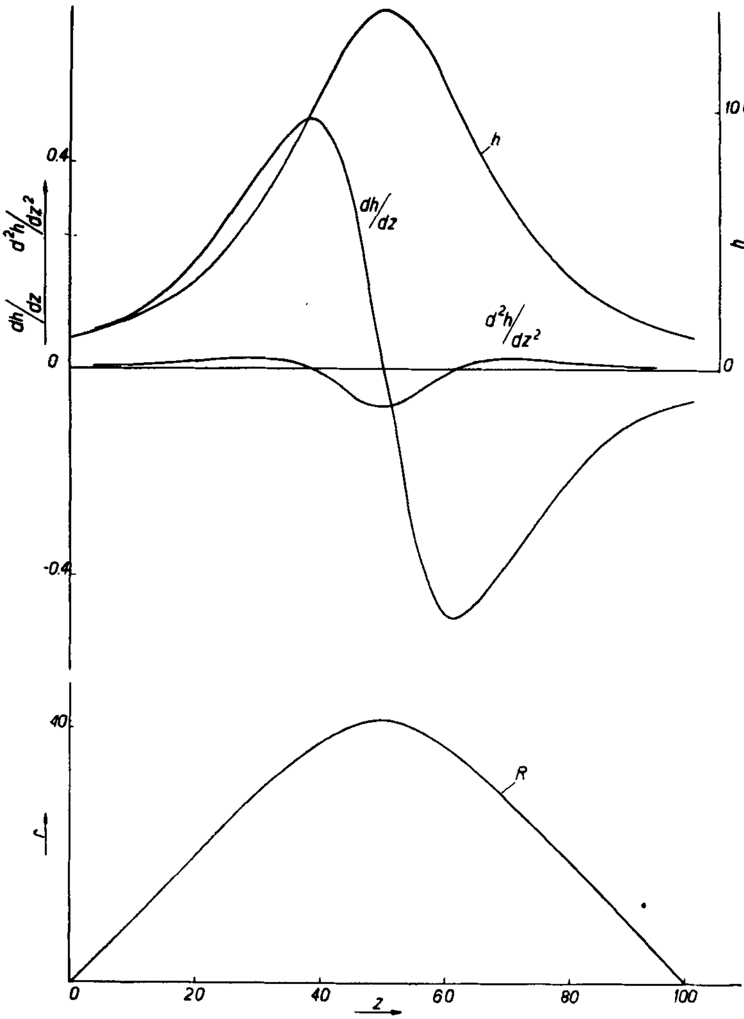

Fig. 5. The measured magnetic field $h(z)$ and its derivatives. The calculated solution $R(z)$ of the first order ray equation.

The accuracy obtained in our case was better than 5.10^{-4} radian tilt angle and 0.5 mm displacement. Irregularities in the field shape can also be detected in this way.

§ 9. *Measurement of the magnetic field,* The magnetic field along the axis has been measured with a flip coil and a creep galvanometer. Absolute values have been obtained by means of a calibrated magnetic etalon in series with the flip coil. The relative accuracy was about 0.1 per cent, the absolute accuracy 1 per cent. The influence of the length of the coil on the measurements, due to the effect of the second derivative of the axial field strength, can in general not be neglected. This can, however, be compensated by a similar effect depending on the radial dimension of the coil. This compensation can be obtained by a suitable coil shape. This will be clear from the following calculation. The total flux through a cylindrical coil with n turns, a radius r and a length $2a$, with its axis along the z-axis and its centre at z_0 is given by

$$\Phi = n/2a \int_{-a}^{+a} 2\pi r\, A_\varphi d(z - z_0).$$

This can be evaluated by using (8):

$$\Phi = n.\pi r^2 [H(z_0) + (a^2/3 - r^2/4)\, H''(z_0)/2 + \ldots].$$

The coil dimensions have to be chosen so that $2a = r\sqrt{3}$. The terms containing H^{IV} will still restrict the coil dimensions.

The result of the field measurements is shown in fig. 5.

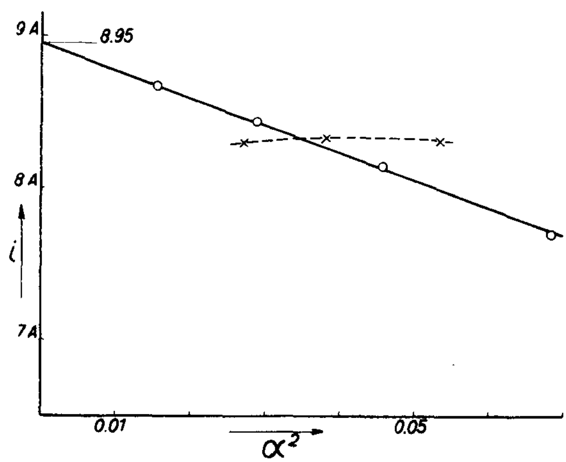

Fig. 6. A measurement of the spherical aberration (0). The measurements of fig. 7 are indicated by (x).
An appreciable reduction in the effect of the spherical aberration has been obtained in the latter case.

§ 10. *Lens strength, spherical aberration and ring focus.* The solution $R_0(z)$ of equation (14) and $R_0'(0) = 1$, $R_0(0) = R_0(100) = 0$, calculated from the measured magnetic field, is shown in fig. 5. The calculated value of the lens constant is: $k_0^2 = 1.063.10^{-5}$. The calculated values of the aberration constants are $C_1 = 140$ cm and $C_2 = 270$ cm.

Measurements of the spherical aberration have been carried out with the ThB F line, $H\varrho = 1385$ eGcm. A source diameter of 0.3 cm and a central exit aperture of the same diameter have been used. The results are given in fig. 6. A straight line is expected if α is on a quadratic scale. The value of C_2/C_1 so obtained is 2.0, in fair agreement with the calculated value of 1.92.

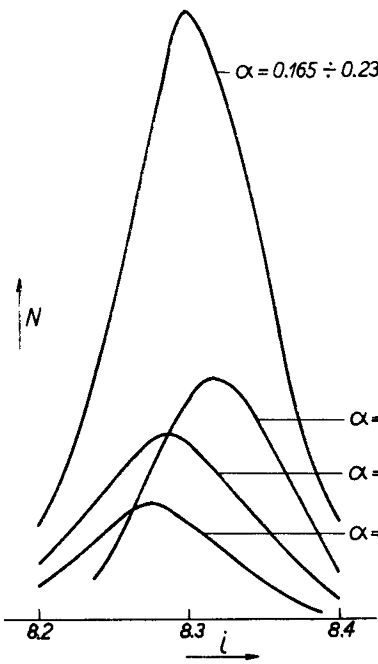

Fig. 7. A measurement of the Th B F line with a ring-shaped exit slit ($r_i = 2.9$ cm, $r_0 = 3.2$ cm, $d = 16$ cm, source diameter 0.3 cm). The value of $\Delta = \Delta(\alpha)$ is shown to have an extreme value (cf. fig. 2). A numerical comparison with (23) is given in table II.

The momentum of the electrons, calculated from the extrapolated current for $\alpha = 0$ and the calculated value of k_0, is 1373 eGcm, in good agreement with the real value.

A ring shaped exit slit of 2.9 cm inner radius and 3.2 cm outer radius has been placed at $z = 84$ cm ($d = 16$ cm) (fig. 3). The small diameter of the counter window (2 cm) has limited the variation in α. Measurements carried out with this focusing slit are represented in fig. 7. This figure clearly shows that $\Delta = \Delta(\alpha)$ passes through an extreme value. These measurements are also plotted in fig. 6, showing the reduction of the influence of the spherical aberration.

An exact numerical agreement with the theoretical formulae cannot be expected due to the approximations introduced when deriving this formulae and also due to the inaccuracy in the determination of the exit angle α. A comparison between these measurements and equation (23) is given in Table II. The adopted values for the spherical and chromatic aberrations are $C_1 = 140$ cm $C_2/C_1 = 2{,}0$.

TABLE II

A comparison between (23) and the measurements shown in fig. 7

Experimental			Theoretical
α	i	Δ	Δ
0.165	8.275	0.075	0.070
0.195	8.315	0.071	0.072
0.230	8.285	0.074	0.085

$C_1 = 140$ cm, $C_2/C_1 = 2.0$, $d = 16$ cm, $M = 1$, $\varrho = 3.05$ cm

§ 11. *Conclusion.* The theory described gives a good description of the behaviour of the electrons in the vicinity of the focal plane of a short magnetic lens. By using the well defined ring-shaped focus the resolving power of a lens type beta ray spectrometer can be greatly improved. The dimensions and the location of this focus for any value of the exit angle can be determined by calculation or experimentally. The theoretical treatment can serve as a guide in the latter case.

The author is very much indebted to Professor C. J. Bakker. Without his much appreciated help and supervision this work could not have been completed.

The spectrometer has been constructed in the machine shop of the Zeeman Laboratory under supervision of Mr. J. van der Zwaal, technical chief of the Zeeman laboratory and of Mr. P. van der Roest, chief of the machine shop. The author is also indebted to Mr. G. J. Nijgh who has done most of the work on the geiger counter and its electronic equipment and who has carried out part of the measurements.

Received July 6th, 1949.

REFERENCES

1) Deutsch, M., L. G. Elliot and R. D. Evans, Rev. sci. Instr. **15** (1944) 178.
2) Siegbahn, K., Arkiv f. Mat. Astr. o Fysik **A30** (1944).
3) Siegbahn, K., Phil. Mag. **37** (1946) 162.
4) Witcher, C. M., Phys. Rev. **60** (1941) 31.
5) Dumond, J. W. M., Rev. sci. Instr. **20** (1949) 160.
6) Persico, E., Rev. sci. Instr. **20** (1949) 191.
7) Zünti, W., Helv. phys. Acta **21** (1948) 179 (A).
8) Zworykin, V. K., G. A. Morton, E. G. Ramberg, J. Hillier and A. W. Vance, Electron optics and the electron microscope, 1st ed., p. 504; New-York, 1945.
9) Busch, H., Ann. Physik **81** (1926) 974.
10) Ments, M. van, and J. B. le Poole, Appl. sci. Res. **B1** (1947) 3.
11) Svartholm, N., Arkiv f. Mat. Astr. o Fysik. **B28** (1942) 16.
12) Glaser, W., Z. Phys. **109** (1938) 700.
13) Verster, N. F., Appl. sci. Res. **B1** (1949) 358.